SUPPLEMENTARY INFORMATION

Engineering shallow and deep level defects in κ-Ga_2O_3 thin films: comparing metal-organic vapour phase epitaxy to molecular beam epitaxy and the effect of annealing treatments

P. Mazzolini,[1,2(*)] J.B. Varley,[3] A. Parisini,[1] A. Sacchi,[1] M. Pavesi,[1] A. Bosio,[1] M. Bosi,[2] L. Seravalli,[2] B.M. Janzen,[5] M.N. Marggraf,[5] N. Bernhardt,[5] M.R. Wagner,[6,5] A. Ardenghi,[6] O. Bierwagen,[6] A. Falkenstein,[4] J. Kler,[4] R.A. De Souza,[4] M. Martin,[4] F. Mezzadri,[7,2] C. Borelli,[1] R. Fornari [1,2]

[1] *Department of Mathematical, Physical and Computer Sciences, University of Parma, Viale delle Scienze 7/A, 43124 Parma, Italy*

[2] *IMEM-CNR, Viale delle Scienze 37/A, 43124 Parma, Italy*

[3] *Lawrence Livermore National Laboratory, Livermore, United States*

[4] *Institute of Physical Chemistry, RWTH Aachen University, D-52056 Aachen, Germany*

[5] *Technische Universität Berlin, Institute of Solid State Physics, Hardenbergstr. 36, 10623 Berlin, Germany*

[6] *Paul-Drude-Institut für Festkörperelektronik, Leibniz-Institut im Forschungsverbund Berlin e.V., Hausvogteiplatz 5-7, 10117 Berlin, Germany*

[7] *Department of Chemistry, Life Sciences and Environmental Sustainability, University of Parma, Viale delle Scienze 17/A, 43124 Parma, Italy*

[(*)] *piero.mazzolini@unipr.it*

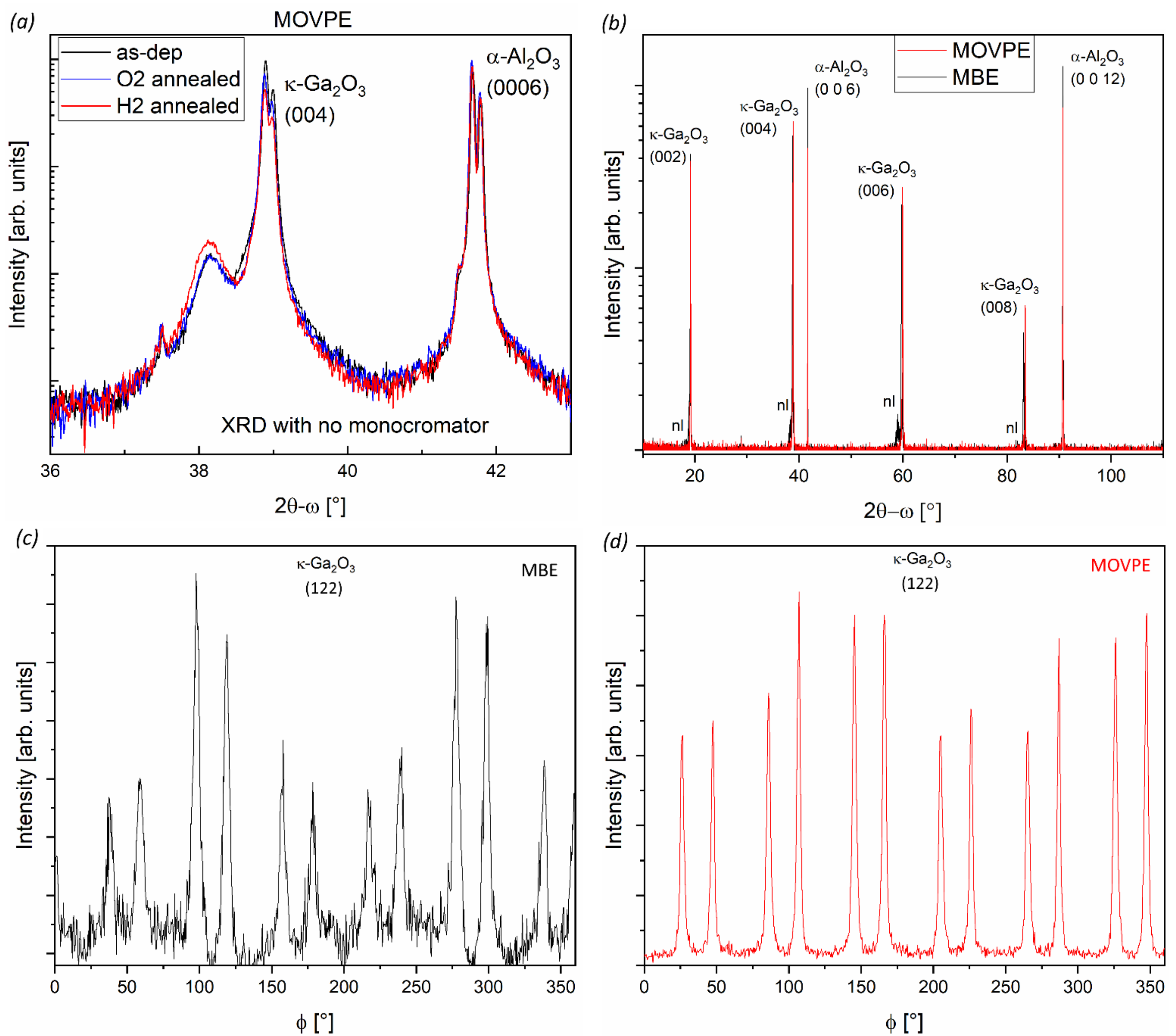

Figure S1 (a) XRD of the MOVPE layers before and after ex-situ thermal treatments collected with non-monochromatic Cu $K\alpha_{1,2}$ incident beam. The diffraction patterns [here a detail referred to the most intense (004) κ-Ga_2O_3 is reported] show no detectable changes upon annealing. (b) Extended 2θ-ω scan (10°-110° using monochromatic Cu $K\alpha_1$ incident beam) for both MBE and MOVPE as-deposited layers showing the (001) epitaxial growth of κ-Ga_2O_3 over the c-plane sapphire substrate. The "nl" label indicates the epitaxial (-201)-oriented β-phase nucleation layer for the MBE-grown film. (c, d) report the φ-scans referred to the (122) reflection of the κ-Ga_2O_3 layers deposited by MBE and MOVPE, respectively; both layers show the presence of twelve peaks in the φ-scans generated by the presence of 120° in-plane rotated domains [a single domain layer would show for the φ-scan of the (122) reflection just four peaks].

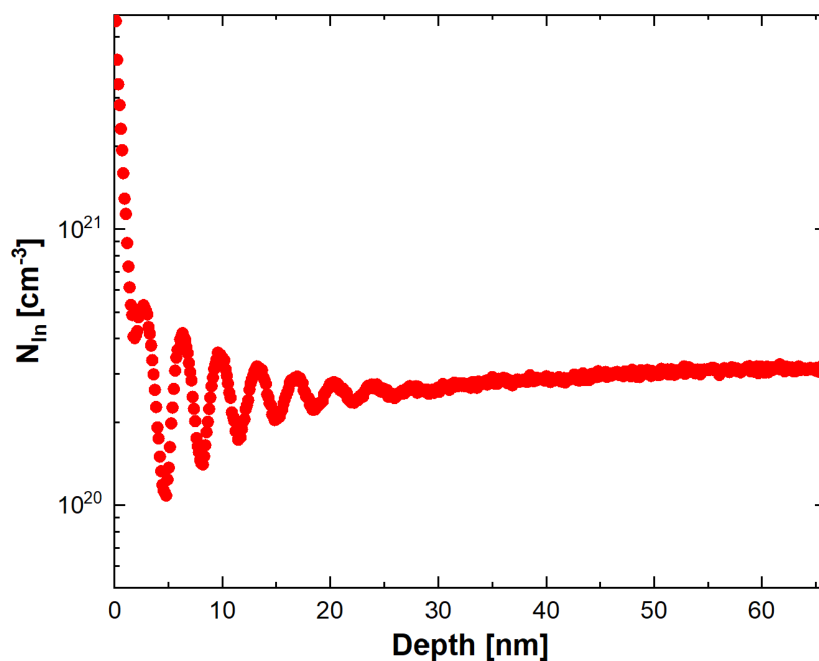

Figure S2 SIMS profile of In in the MBE deposited sample. The fluctuation in the In signal close to the layer surface were repeatable in different measurements performed on this layer; their origin could be related to slight fluctuations of fluxes / T in the very last stages of the MEXCAT-MBE deposition process.

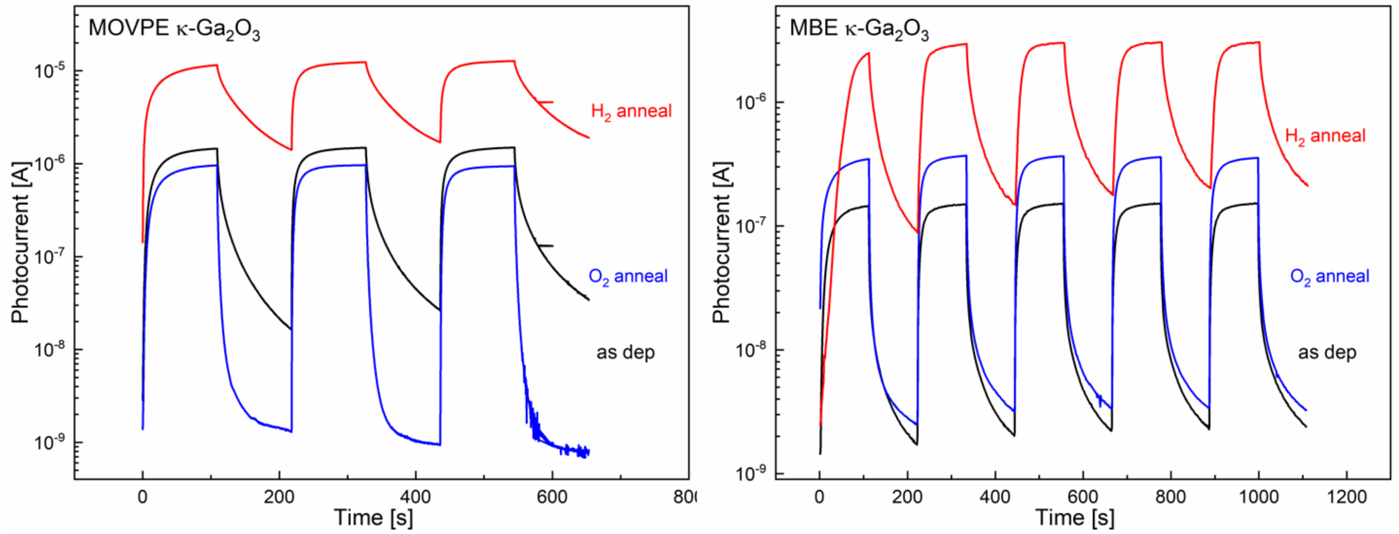

Figure S3 On-off cycles ($\lambda_{On} = 250\ nm$, $t_{on-off} = 110\ s$) for PDs based on MOVPE and MBE material. The normalized cycles reported in the manuscript are referred to the 3rd cycle.

The cycles reported in Figure S3 show that the chosen delay time is not leading to a plateau in both the on and off recorded currents; therefore, a current pile-up is especially visible in the dark current upon cycle iteration. This is not an irreversible effect, *i.e.*, without being exposed to the $\lambda_{On} = 250\ nm$ for longer times eventually decades to the originally recorded dark currents.

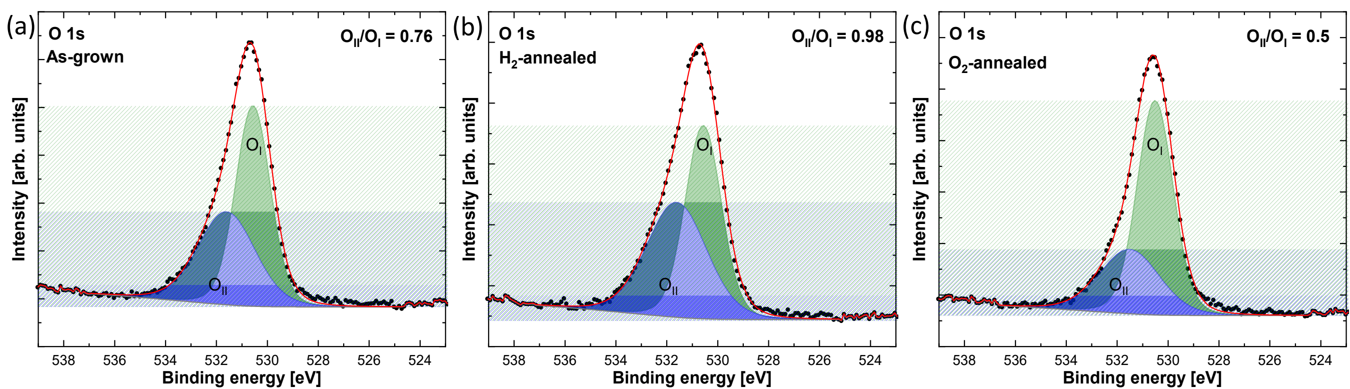

Figure S4 XPS O1s core level spectra for (a) as-deposited, (b) H_2-, and (c) O_2-annealed MOVPE layers.

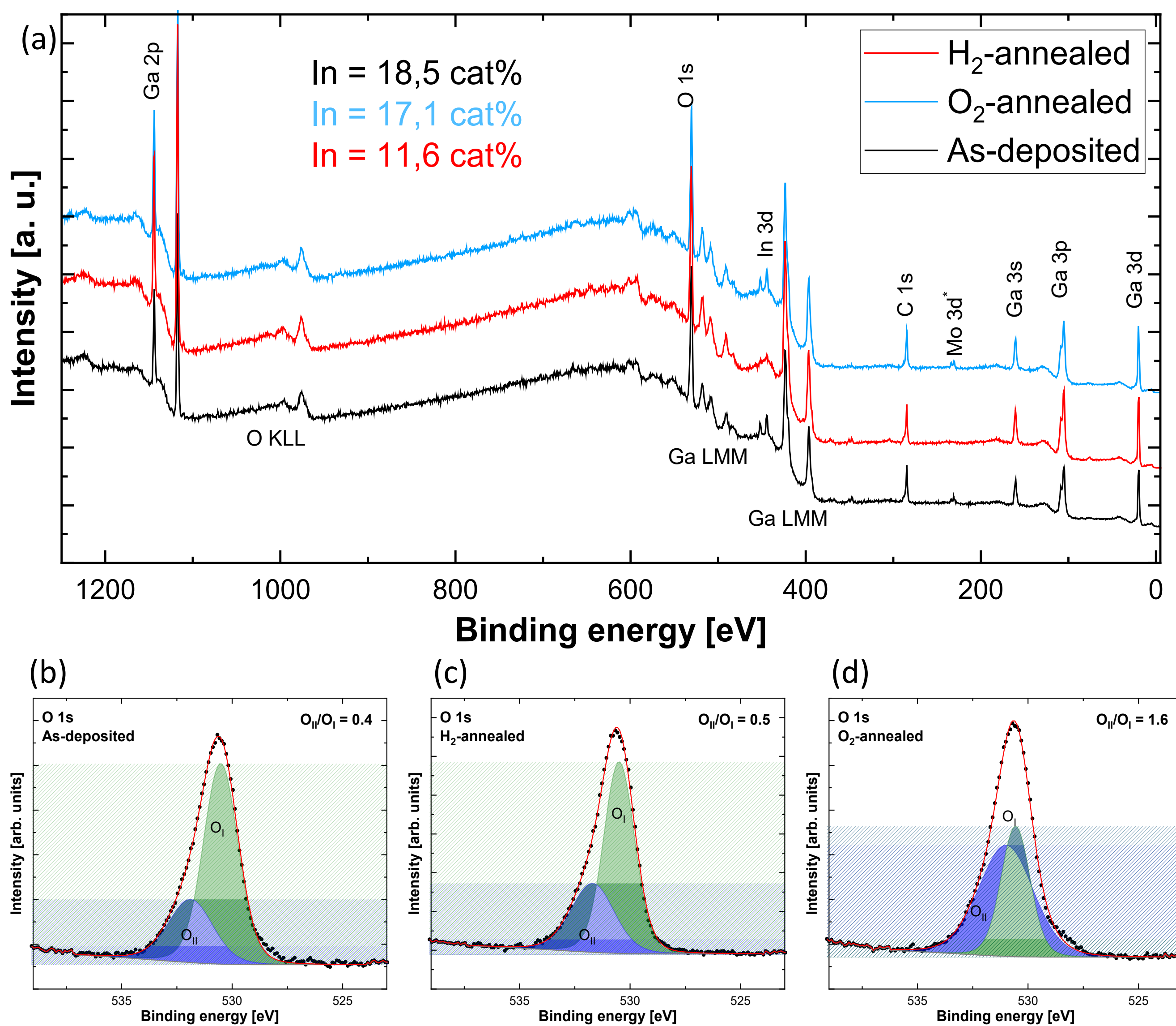

Figure S5 (a) Survey scan for the MBE grown layer showing the presence of In at the surface, the small signal for Mo is arising from the clip to hold the sample; the In cat. % reported in the inset were calculated from the XPS data using the ratios of the Ga 2p and In 3d areas corrected for their respective relative sensitivity factors (RSF) and our specific experimental setup (*i.e.,* angle between source and analyzer and transmission function). (b) O1 s peak for the MBE as-deposited, (c) H_2-annealed and (d) O_2-annealed. Due to the presence of In/In_2O_3 at the surface the In-O bond will affect the overall O1 s shape.

Table S1 Kinetic energy, IMFP and escaping depth for Ga $2p_{3/2}$ O 1s, Ga 3s and VBM in κ-Ga_2O_3 calculated using the TPP-2M equation.[2]

	Kinetic energy eV	IMFP Å	3λ Å
Ga $2p_{3/2}$	346,4	10,3	30,9
O 1s	933,7	20,7	62,1
Ga 3s	1303,7	26,8	80,4
VBM	1477,1	29,5	88,5

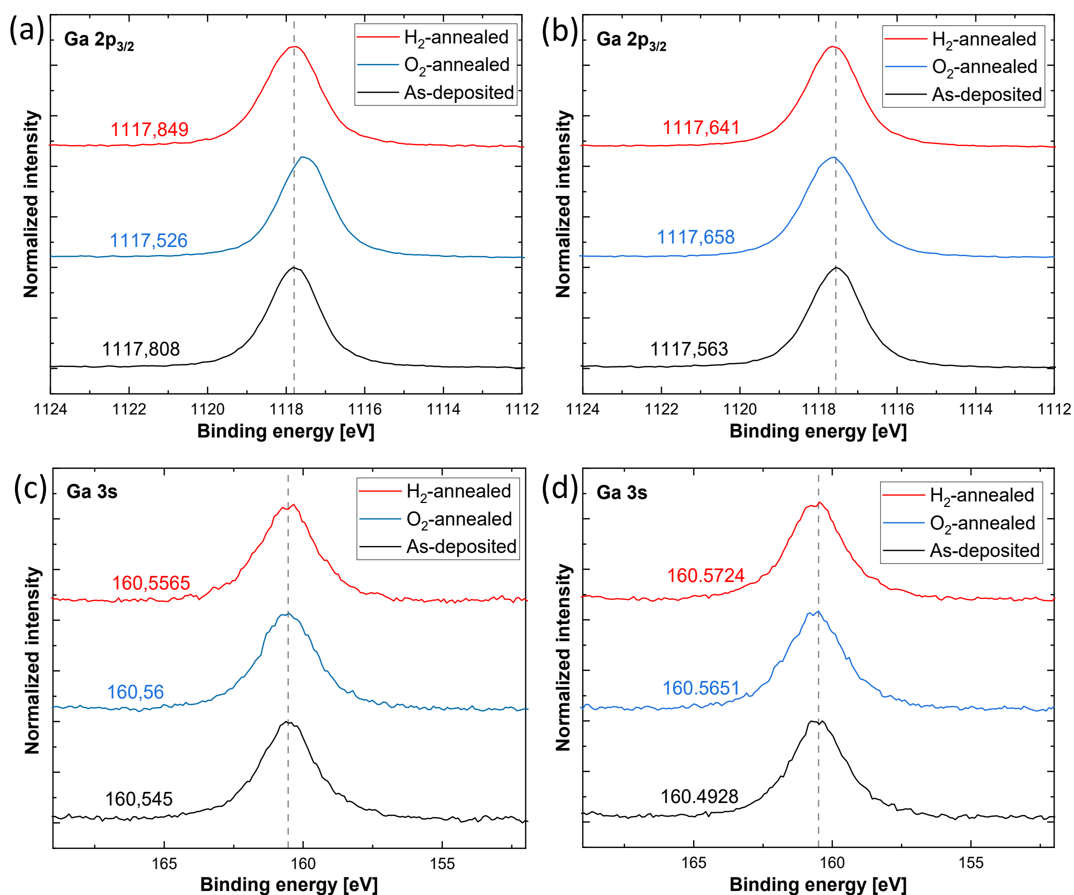

Figure S6 Comparison between the Ga $2p_{3/2}$ and Ga 3s core levels between the as-grown, O_2-annealed and H_2-annealed for the MOVPE sample (a) and (c) and for the MBE sample (b) and (d).

In Table S1 we show the predicted inelastic mean free path (IMFP) and the escaping depth (3λ) for κ-Ga_2O_3 as a function of the kinetic energy highlighting the more surface sensitive nature of the Ga $2p_{3/2}$ peak compares to the more "bulk"-like Ga 3s peak. Figure S6 shows the chemical shift for this two Ga core levels. While for the Ga $2p_{3/2}$ peak some shift can be observe in comparison to the as-grown sample, this shift becomes neglectable once we look at the Ga 3s, highlighting how these variations are mostly related to surface effects.

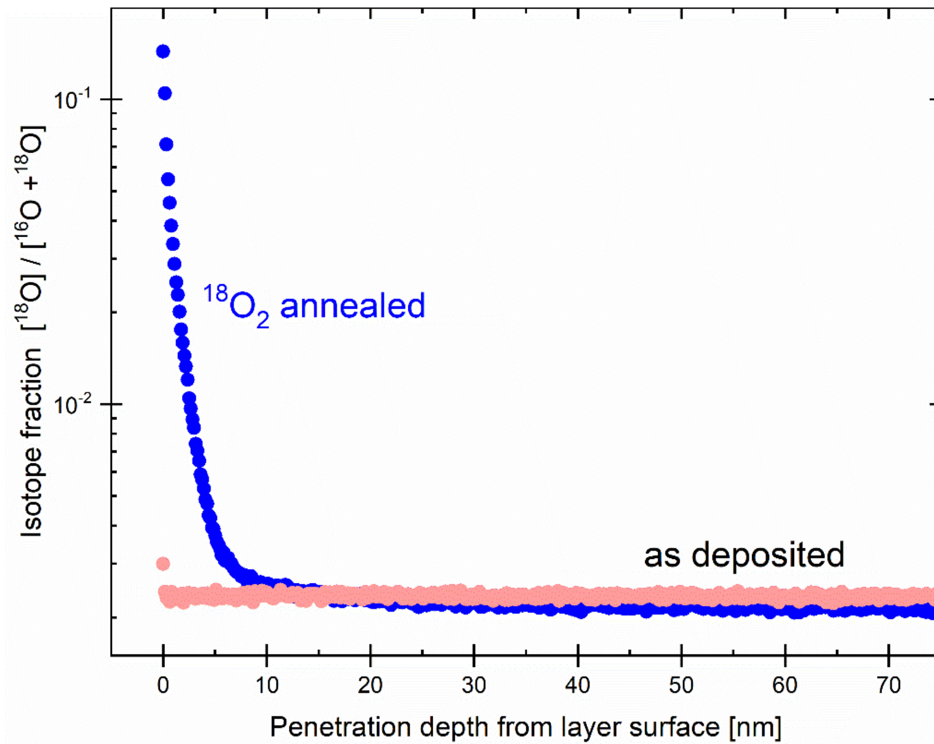

Figure S7 ToF-SIMS depth profile of the ^{18}O isotope fraction for an as-deposited (pink) and $^{18}O_2$-annealed MOVPE layer.

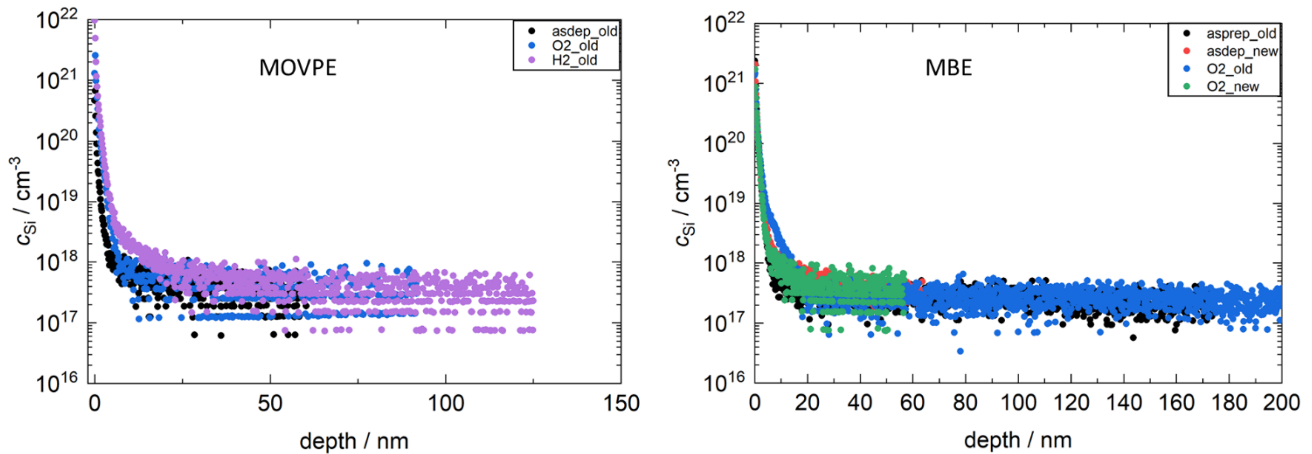

Figure S8 Si quantification (through β-Ga_2O_3 Si implantation standard, see reference[1]) through ToF-SIMS depth profiling of as deposited and annealed MOVPE and MBE samples. The suffix "old" and "new" represent different measurements performed on the layers; in the case of the MBE layers, they show the good reproducibility of the

acquired data (old - new). As Si is a well-known surface contaminant, the higher concentration at the surface (< 20 nm) should not be considered. All of the samples fall in the same background level, just at the edge of the detection limit.

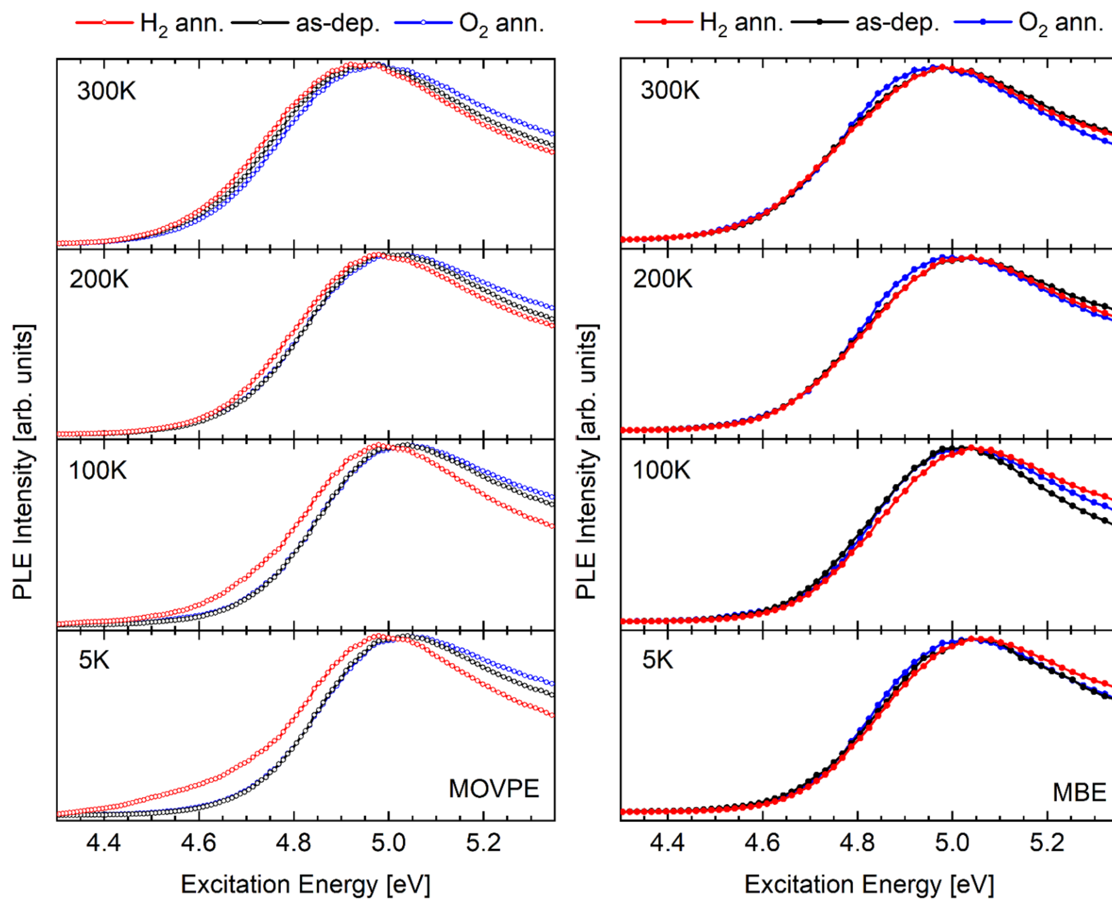

Figure S9 Temperature dependent PLE of MBE (left) and MOVPE (right) grown kappa-Ga_2O_3 samples for detection energies between 1.8 eV to 4.0 eV.

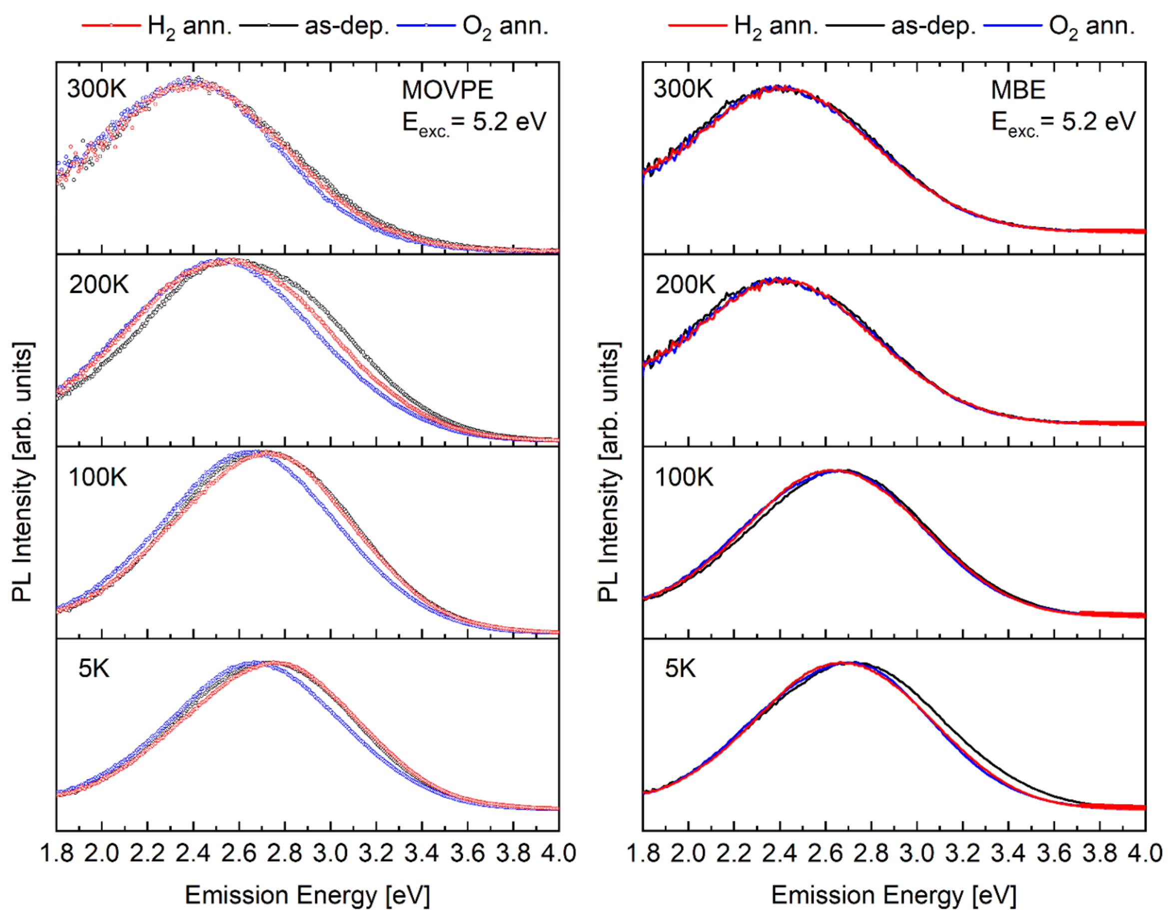

Figure S10 PL spectra of as-deposited, O_2, and H_2 annealed MOVPE and MBE κ-Ga_2O_3 thin films measured at temperatures of T = 5K, 100K, 200K, and 300K. Spectra are shown for above band edge excitation at 5.2 eV.

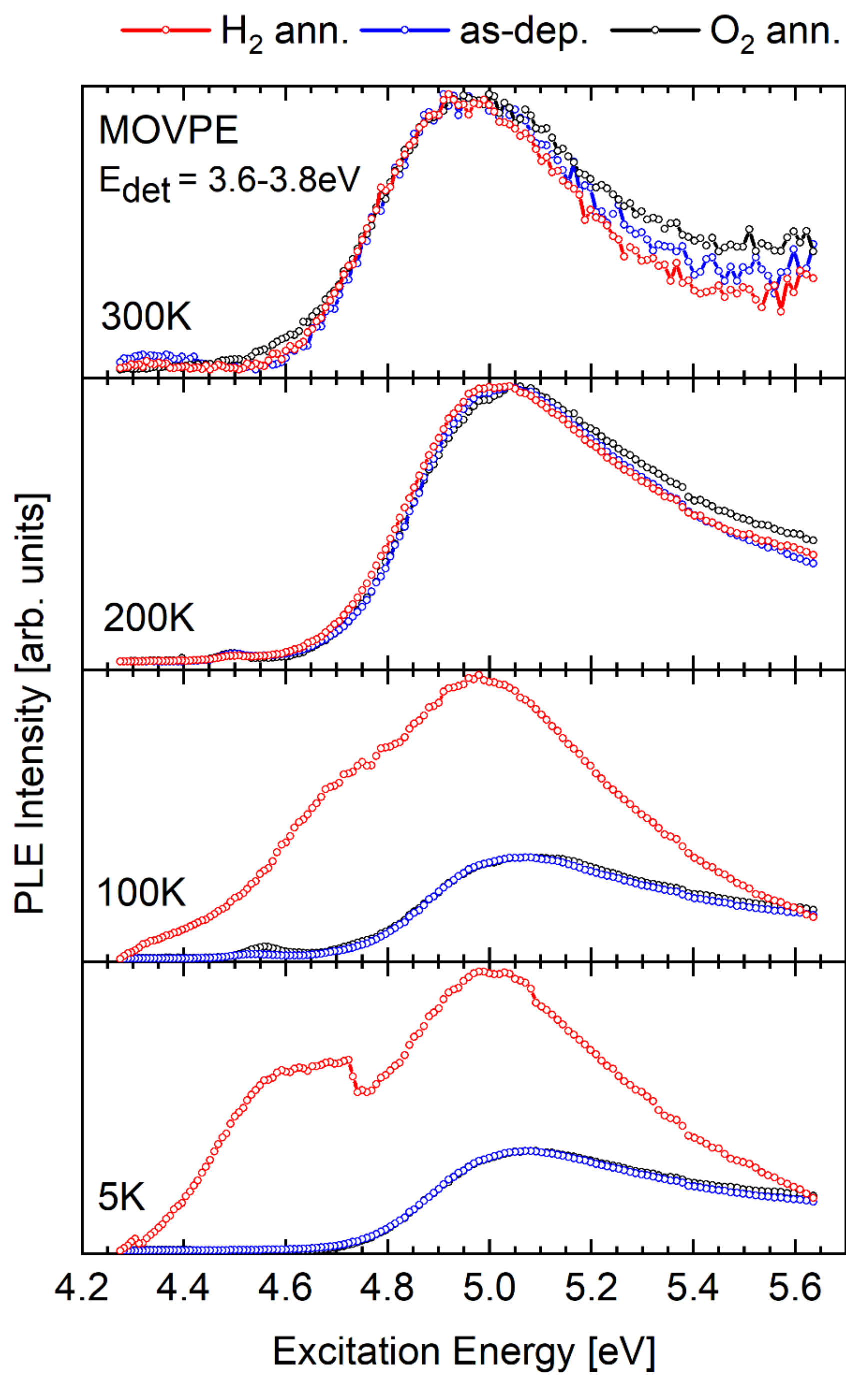

Figure S11 Temperature dependent excitation spectra of MOVPE grown κ-Ga_2O_3 samples for a detection energy of 3.6 eV to 3.8 eV.

Table S2 Summary of calculated charge-state transition levels as defined relative to the valence band maximum (VBM) for isolated vacancies on the different distinct lattice sites in the κ-phase as described in the text. We also include levels for hydrogen-related complexes that were calculated, including the only HO that exhibits a deep level (H_{O6}) and the hydrogenated V_{Ga} that still exhibit deep acceptor states. We omit the (+/0) polaronic states for the hydrogenated V_{Ga} complexes, as these exhibit a spread of defect levels ~1 eV from the VBM depending on the configurations and sites of the oxygens that localize the polaron and bind the proton at the vacancy. All values in eV.

Defect	(+2/0)	(+2/+)	(+/0)	Defect	(+/0)	(0/–1)	(–1/–2)	(–2/–3)
V_{O1}	3.93	3.97	3.90	V_{Ga1}	1.21	1.43	2.37	2.51
V_{O2}	3.03	3.04	3.02	V_{Ga2}	0.92	1.18	2.08	2.65
V_{O3}	3.75	4.09	3.40	V_{Ga3}	1.01	1.56	2.33	2.67
V_{O4}	3.63	4.26	3.00	V_{Ga4}	0.92	2.12	2.26	2.58
V_{O5}	3.77	4.14	3.40	V_{Ga}^{i}	1.11	1.42	1.69	1.84
V_{O6}	2.90	3.62	2.18	H_{O6}	--	3.96	--	--
Defect	(0/–1)	(–1/–2)		Defect	(0/–1)			
V_{Ga1}-H	1.31	2.15		V_{Ga1}-2H	1.40			
V_{Ga2}-H	1.75	2.21		V_{Ga2}-2H	0.82			
V_{Ga3}-H	1.43	2.43		V_{Ga3}-2H	1.36			
V_{Ga4}-H	1.84	2.22		V_{Ga4}-2H	1.85			
V_{Ga}^{i}-H	1.46	1.84		V_{Ga}^{i}-2H	1.38			

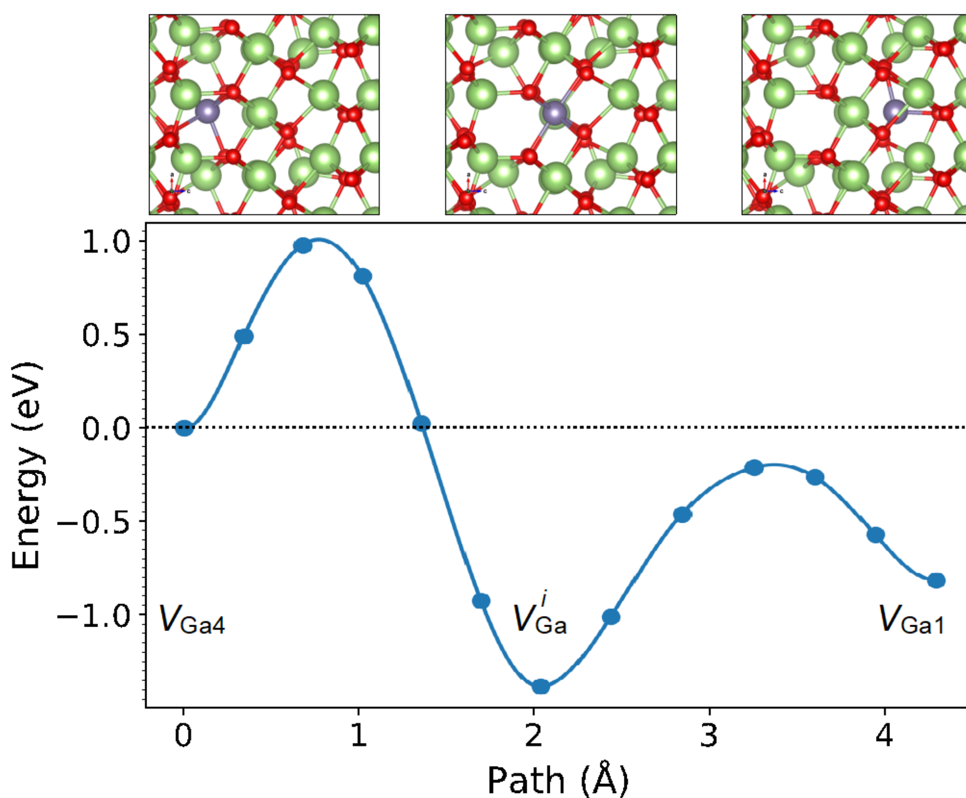

Figure S12 Plot of the calculated migration pathway for a V_{Ga}^{-3} between a distorted octahedral site (Ga4) and a tetrahedral site (Ga1), where a split-vacancy configuration (V_{Ga}^{i}) is found to be more favorable by ~1.5 eV relative to the V_{Ga4}.

References

[1] A. Ardenghi, O. Bierwagen, A. Falkenstein, G. Hoffmann, J. Lähnemann, M. Martin, and P. Mazzolini, "Toward controllable Si-doping in oxide molecular beam epitaxy using a solid SiO source: Application to β-Ga_2O_3," Appl. Phys. Lett. **121**(4), 042109 (2022).

[2] C.J. Powell and A. Jablonski, NIST Electron Inelastic-mean-Free-Path Database, Version 1.2, SRD 71, National Institute of Standard and Technology, Gaithersburg, MD (2010).